Design and Manufacture of an Attachment Fitting for Transtibial Prosthetic Sockets Using Selective Laser Sintering

Danny Burhan and Richard Crawford
Laboratory for Freeform Fabrication
The University of Texas at Austin

Abstract

The focus of this work is using selective laser sintering to manufacture transtibial prosthetics sockets with compliant features to relieve contact pressure in sensitive areas. Each of these sockets requires an integrated attachment fitting to connect to the pylon and foot using standard hardware. Several design concepts of an attachment fitting are presented and compared. The design concepts were tested using a tensile test machine and analyzed using ground reaction force data to ensure a structurally sound connection. The resulting design employs standard hardware while maintaining the integrity of the connection for a normal gait cycle.

Introduction

In United States there is a growing need to fabricate prosthetic sockets faster and more economically, with more than 500,000 current lower extremity amputees and at least 60,000 new ones each year [1]. Conventional methods of fabricating prosthetic sockets are time consuming and expensive, and highly dependent on the skills of prosthetists, of whom there are fewer compared with the number of amputees. The University of Texas at Austin, in collaboration with the Department of Rehabilitation Medicine at the University of Texas Health Science Center at San Antonio (UTHSCSA), is developing an alternative method of fabricating prosthetic sockets that can improve efficiency in prosthetic care, enhance comfort and fit, and reduce time and cost.

The sockets are produced using Selective Laser Sintering (SLS), which creates complex objects by adding and bonding materials in layers. SLS has the capability of forming any complex geometry without the need for elaborate machine setup or final assembly. Using SLS, prosthetic sockets can be created directly from digital shape information, eliminating the need for extensive molds, hand lamination and finishing procedures. SLS also simplifies the construction of complex objects into a manageable, straightforward, and relatively fast process.

Previous research on fabricating subject specific prosthetics sockets using selective laser sintering has been presented by Stevens [2] and Faustini [3]. The process was aimed specifically at the production of patellar- tendon bearing (PTB) sockets, modified with compliant features to relieve contact pressure at certain areas. Figure 1 shows a diagram of a prosthetic limb. The prosthetic limb consists of the socket with integrated attachment fitting, pylon and prosthetic foot. Designing an integrated attachment fitting to mate with standard hardware is the objective of this research.

Objectives

Figure 1 shows that the attachment fitting provides the connection between the socket and pylon. In previous work, the design of the attachment fitting used custom parts, which makes it harder to commercialize the product due to the increase in production cost. The purpose of this research is redesigning the attachment fitting to incorporate standard hardware while maintaining the integrity of the socket and a strong connection to the pylon. Utilizing the advantage of SLS to create complex objects without additional tooling, an integrated attachment fitting will be created.

The research began by setting the design requirements, and then several design alternatives were developed and evaluated. The selected design concept was tested using a tensile test machine and analyzed using applied ground reaction forces (GRF) to ensure a strong connection is achieved.

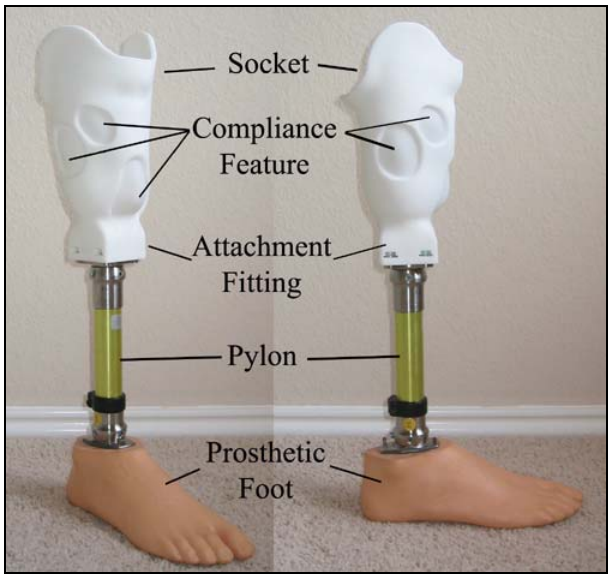

Figure 1: Prosthetic Limb.

UTHSCSA Attachment Fitting Design

UTHSCSA has developed an alternative method of attaching the pylon to the socket. In order to eliminate the use of custom parts, UTHSCSA uses a standard four hole European adaptor, as shown in Figure 2a. This type of adaptor has been used regularly to attach the pylon to conventional sockets and is easily obtainable from any prosthetic hardware vendor. The adaptor is then connected to a standard cylindrical connector (Figure 2b) that enables adjustment of the alignment angle. The adjustment is made by tightening and loosing four setscrews on the outer wall of the connector. Figure 2c is a representation of how the adaptor and connector are joined once the adjustment is made on the definitive socket.

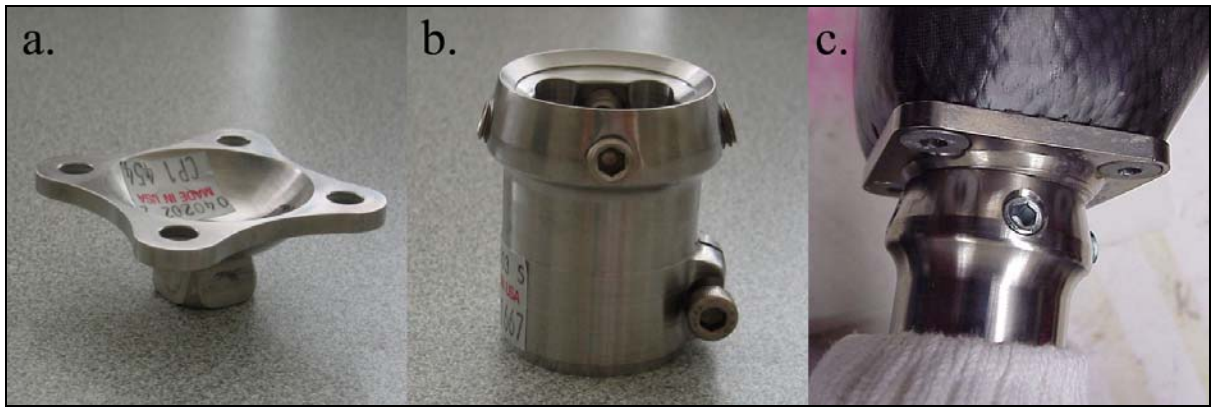

Figure 2: (a) Standard Four Hole European Style Adaptor; (b) Standard Connector; (c) Adaptor Joined to Connector.

For SLS sockets, UTHSCSA designed an integrated attachment fitting to mate with the adapter. The design is simple; a square block is created on the bottom of the socket and united to the socket by using a "blend" operation in the CAD software, creating one continuous smooth surface. In order to secure the adaptor, two small aluminum blocks with internal threads are inserted and tightened using standard 6mm bolts (Figure 3). These aluminum inserts are used because UTHSCSA did not believe that creating direct tapped holes in Duraform^{TM} PA would be possible. Although the UTHSCSA attachment fitting design utilizes standard prosthetic hardware, the design is not completely standard. Even though the cost of manufacturing the custom aluminum blocks is inexpensive, it is not widely available off the shelf. Moreover, the UTHSCSA attachment fitting has not been analyzed or optimized.

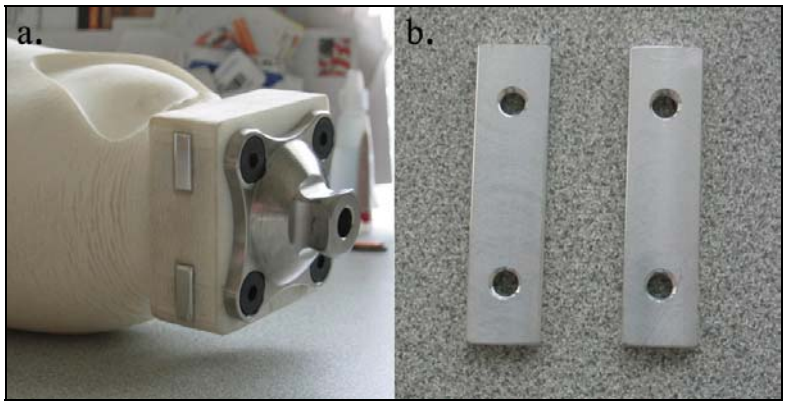

Figure 3: (a) UTHSCSA Attachment Fitting; (b) Aluminum Block Inserts.

Attachment Fitting Design Requirements

The requirements for design of the attachment fitting were set by Gordon Bosker and Bill Rogers [4] from UTHSCSA. As mentioned previously, the usage of all standard hardware is very important for the success of the design. Using standard hardware will improve marketability of the SLS socket throughout the United States and the world. The following are design requirements for the attachment fitting:

1. The design should use the standard four hole European style adaptor (Figure 2a) for the design, since this adaptor will provide adjustment for the alignment angle.

2. The inner profile surface of the socket should be maintained, meaning the fitting should not cause any alterations. The inner profile has been rectified by the prosthetist so that contact pressure is distributed in areas that are less sensitive.

3. The overall shape of the socket should be aesthetically appealing. The attachment fitting should blend smoothly to the socket and should not be too bulky, as this will increase the overall weight of the socket.

4. The attachment fitting should allow the adaptor to be removed when necessary, which means that the adaptor should not be glued permanently to the socket.

5. The use of other standard prosthetic hardware is recommended. This hardware usually is attached to the conventional socket using epoxy. Other standard or universal hardware that is easily accessible is also recommended.

6. The attachment fitting should withstand a normal walking force.

7. The design should not require manufacture of non-standard parts.

8. Fabrication of the attachment fitting should be compatible with SLS.

9. Duraform^{TM} PA should be used as the material for the attachment fitting.

Attachment Fitting Concept Generation

Based on the design requirements, several attachment fitting concepts were created using standard hardware. Figure 4 shows several of these possibilities. Figure 4a shows two of the aluminum inserts that are currently used by UTHSCSA. Figure 4b is a 6mm flange nut, a standard metric nut for a 6mm prosthetic bolt. Figure 4c is a T-insert, usually used in wood, but also a possible insert for Duraform^{TM} PA. Figure 4d is a helicoil, normally used for thread repair. The helicoil works by expansion of its threads after a 6mm bolt is inserted. Figure 4e shows a tap that would be used to create a threaded hole directly in the SLS material. No previous studies have been performed to test the strength of direct tapped holes in Duraform^{TM} PA.

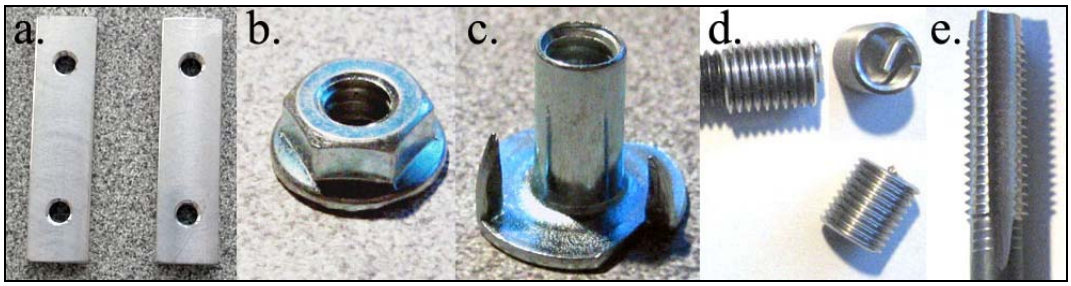

Figure 4: Standard Metal Inserts.

Each of the concepts using standard hardware was refined to determine exactly how the hardware would mate with the socket and the adaptor. As a start, the base of the UTHSCSA attachment fitting (measuring 60mm x 60mm x 16mm) was used (Figure 3a), since it was known to provide solid support for the adaptor. For the flange nut, the attachment fitting is designed around the shape of the nut itself. Figure 5b shows the proposed attachment fitting using the flange nut design. The flange nut is inserted from the side. Once the nut is inside, the wall around the flange nut secures the nut as the bolt is tightened. The adaptor is then installed the same way as it is in UTHSCSA design, directly underneath the socket.

Just like the flange nut design, the T-insert attachment fitting is designed around the insert itself (Figure 5c). The T-insert is inserted from the bottom and glued using epoxy. The spikes in the t-insert will prevent any rotational movement when the bolt is tightened. A feasibility study of gluing metal to Duraform™ PA was performed to ensure that a bond to Duraform™ PA can be formed. The study consisted of gluing the flat side of the t-insert to Duraform™ PA using an all-purpose epoxy. Before gluing, the surface of the plate was cleaned thoroughly to remove loose powder. The result shows that gluing metal objects to Duraform™ PA is a feasible alternative.

Attachment fitting designs for the helicoil insert and the direct tapped holes are straightforward (Figure 5d). The base of the socket where the adaptor is connected is the same as for the flange nut and T-insert designs. Both of the designs require drilling holes for the 6mm helicoil insert and the 6mm direct tapped hole. A special tap is required for inserting the 6mm helicoil and the required hole for this tap is 0.25". Once the holes have been tapped, the helicoil is then inserted using a special tool. After the helicoil reaches the desired depth, the special tool cuts off the tip of the helicoil, clearing the path for the bolts to be inserted. For the direct tapped hole, a regular 6mm tapped hole is required. Once the hole has been tapped the bolts are inserted normally.

Four of these refined designs were presented to UTHSCSA staff. All of the designs are simpler and use standard commercial hardware. UTHSCSA staff recommended testing each of the concepts. Each of these concepts was compared to the UTHSCSA design. The results of these tests are presented below.

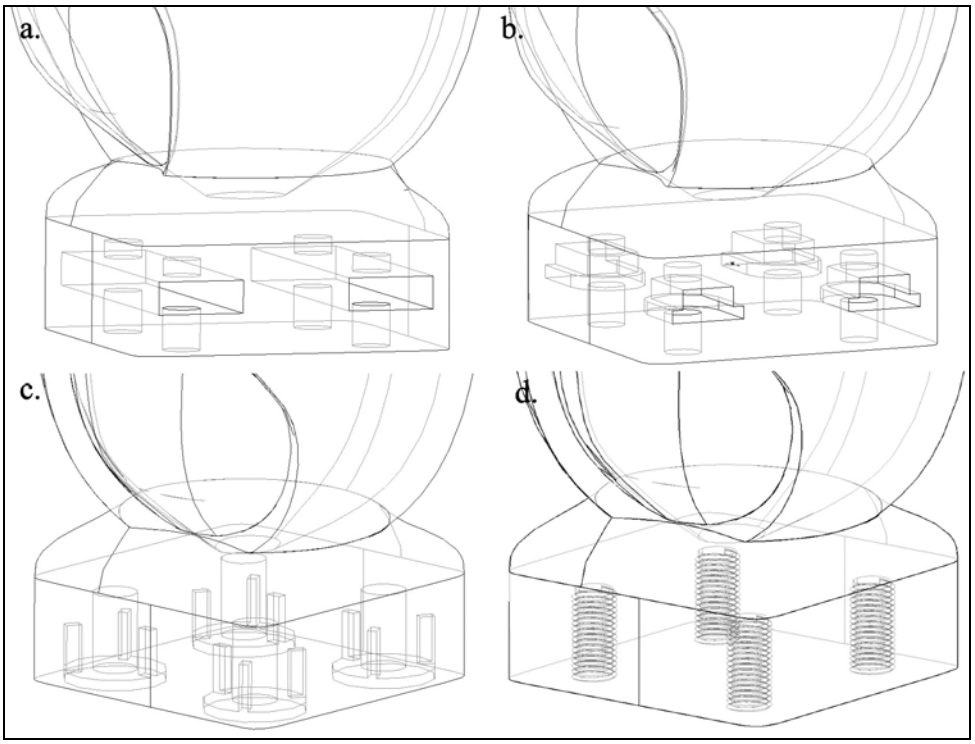

Figure 5: (a) UTHSCSA Attachment Fitting Design; (b) Flange Nut Attachment Fitting Design; (c) T-insert Attachment Fitting Design; (d) Helicoil and Direct Tapped Attachment Fitting Design.

Concept Selection

To test and compare the concepts, a MTS 810 tensile test machine was used. The machine has two spring-loaded grips that are normally used to hold "dogbane" tensile specimens. The grip has a maximum opening of 17mm; therefore, the specimen needs to have a maximum width of 17mm. To accommodate the width of the grip, a custom specimen for each concept was needed (Figure 6). Each specimen was created based on the location of probable failure. Analyzing the UTHSCSA and flange nut design, the strength of the design depends on the sidewall of the holes. For the T-insert, the strength depends on the bonding strength of the epoxy glue, and for the helicoil, the strength depends on the wall thread of the helicoil. Therefore, testing one corner of a complete attachment fitting, which includes just one hole, is sufficient since this reflects the strength of each individual design.

For the test, a total of twenty-five specimens were built, five specimens for each concept. The testing follows ASTM Standard D638-02a procedure for testing polymer material in tension. Although the specimen dimensions do not comply with the specifications of the standard, the procedures in the testing do follow steps in the standard. A feed rate of 5mm/min was chosen based on the standard. The results of the testing are summarized in Table 1. The table lists the tensile force required to break the specimens in pounds-force (lbf). It also lists the average and the range for each concept. The range for the design is included to indicate the consistency of the test. As can be seen in the table, two of the direct tapped specimens did not provide good

results and were not recorded. This was probably due to poor tapping, which indicated that the same mistakes could occur if the direct tap design was chosen as the selected concept. For this reason, the direct tap design was immediately eliminated as one of the concepts.

Table 1: Tensile Test Force Results (lbf).

Test	Flange	UTHSCSA	T-Insert	Helicoil	Direct Tapped
1	1304.42	1401.91	566.81	1154.78	365.78
2	1166.12	1370.93	756.50	1123.04	442.11
3	1230.36	1433.65	659.01	1287.80	487.46
4	1237.92	1433.65	466.30	1164.61	—
5	1203.91	1445.75	157.20	1165.36	—
Average	1228.54	1417.18	521.16	1179.12	431.78
Range	138.30	74.82	599.31	164.75	76.33

Figure 6 shows the failure location for each specimen. As predicted, all UTHSCSA and flange specimens failed at the sidewall, since this is the weakest point of the design. For the T-insert design, the failure occurred when the insert was fully extracted out of the base, whereas the helicoil and direct tapped failed when the Duraform™ PA threaded wall was completely stripped out. The result of the testing indicates that the UTHSCSA design is the strongest. Also, the range of the UTHSCSA concept is smallest, indicating the test was consistent. Theoretically, the flange design should be stronger than UTHSCSA design since it has a larger sidewall cross-sectional area, but the results from the test indicate the contrary. This issue is discussed below. The results for the T-insert design are very inconsistent since these data have the largest range. The strength of the T-insert design is highly dependent on the amount of epoxy in contact with the wall of the hole and the insert. The amount of epoxy that was applied was very difficult to control in every specimen, and resulted in inconsistent test results. The test results for the helicoil design were consistent and showed good strength. Even though the helicoil is not the strongest design, it does prove that the helicoil improves the strength of a threaded hole in Duraform™ PA compared to a direct tapped hole.

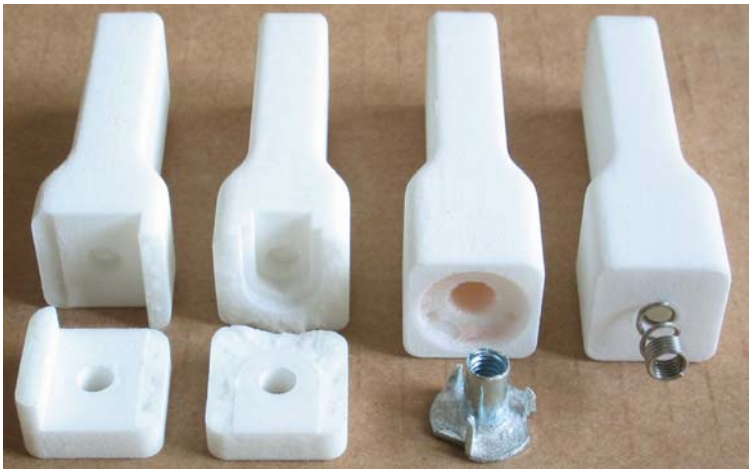

Figure 6: Condition of Test Specimens after Testing.

The test results do not give a definitive answer in terms of which concept is strongest. The UTHSCSA and flange designs were stronger than any other designs, but because of the counterintuitive results from the test, further testing was needed to determine what actually happened. The flange nut design was suspected to have lower strength because of its build location in the SLS workstation. All of the flange nut specimens were built in the front part of the build cylinder, whereas the UTHSCSA specimens were built towards the back. Build location can be a factor in determining strength, since there are several heaters in the SLS workstation and the temperature of these heaters can vary, thus affecting the strength of the part [5]. To test this hypothesis, a new set of UTHSCSA and flange specimens were fabricated with the build locations switched.

Because of problems with the MTS 810 tensile machine, an Instron Tensile Machine was used for the second set of tests. Since the Instron's grip is smaller and narrower than the MTS 810 grip, the previous specimens did not fit in the Instron's grip. To verify whether build location plays a role, a simpler approach was pursued. Instead of testing the concept specimens made earlier, standard dogbanes were tested. Ten dogbanes were built and tested based on ASTM Standard D638-02a. Five of them were built in the front of the build cylinder and the other five in the back. The results of the test are summarized in Table 2.

Table 2. Dog bones Test Results.

Specimen	**Max Load (lbf)**	**Specimen**	**Max Load (lbf)**
Front - 1	175.35	Back - 1	254.03
Front - 2	182.10	Back - 2	240.55
Front - 3	211.32	Back - 3	224.81
Front - 4	218.06	Back - 4	200.08
Front - 5	220.31	Back - 5	220.31
Average	**201.43**	**Average**	**227.96**
Range	**47.96**	**Range**	**53.95**

The test results show that the specimens built in the back of the build cylinder were stronger than the ones in the front. These results support the explanation of why the flange design specimens were weaker. The flange design should perform as well as the UTHSCSA or even better. Based on the result of the dog bone tensile test results, the flange nut design was selected as the attachment fitting for the SLS prosthetic socket. Under ideal conditions, the flange nut design should perform slightly better than UTHSCSA design.

Testing the Complete Attachment Fitting

After selecting the flange nut design as the attachment fitting, the strength of the whole attachment fitting was evaluated, assuming the attachment fitting is the weakest point in the prosthesis. Figure 5b was used as a starting design for testing the attachment fitting. Since other areas of the socket that are more susceptible to failure than the fitting, testing the whole socket with the attachment fitting would yield information about the strength of the fitting design. Therefore a specific test specimen was needed. The complete attachment specimen needs to fit in the available tensile test machine, the MTS 810 machine. For this test, using the grips was not

possible since the width of the attachment fitting itself is greater than 17mm. Figure 7a shows the complete attachment fitting specimen and Figure 7b shows the setup for the test. The specimen was made by taking the base feature in Figure 5b and blending it with flange nut design. The upper portion of the specimen accommodates a one-inch threaded shaft coming out of the test machine (See Figure 7b). This shaft is then secured using a one-inch nut and washer. A larger surface area was created for the upper feature to accommodate the one-inch nut and to ensure that the upper feature did not fail first. The bottom part of the specimen was connected to a custom plate with a threaded shaft secured to the specimen using four 6mm bolts.

The test was performed using a 5mm/min feed rate, and the force to break the specimen was 5799.61 lbf (25,797.95 N). This force was more than four times the average individual specimen tested previously, which was 4914.16 lbf. This result is expected since the cross-section of the full attachment fitting is larger than the area of the individual specimen. The test also indicates the location of failure is on the sidewall where the flange nuts are located. Figure 7c also shows the condition of the attachment fitting after failure. The fracture is conical and located at the holes, indicating that stress concentrations appeared before the specimen finally failed. The result of this test was then compared with ground reaction force data of an amputee wearing a traditional prosthetic socket. Using the GRF data, the attachment fitting was evaluated to determine whether it is strong enough to withstand normal walking forces.

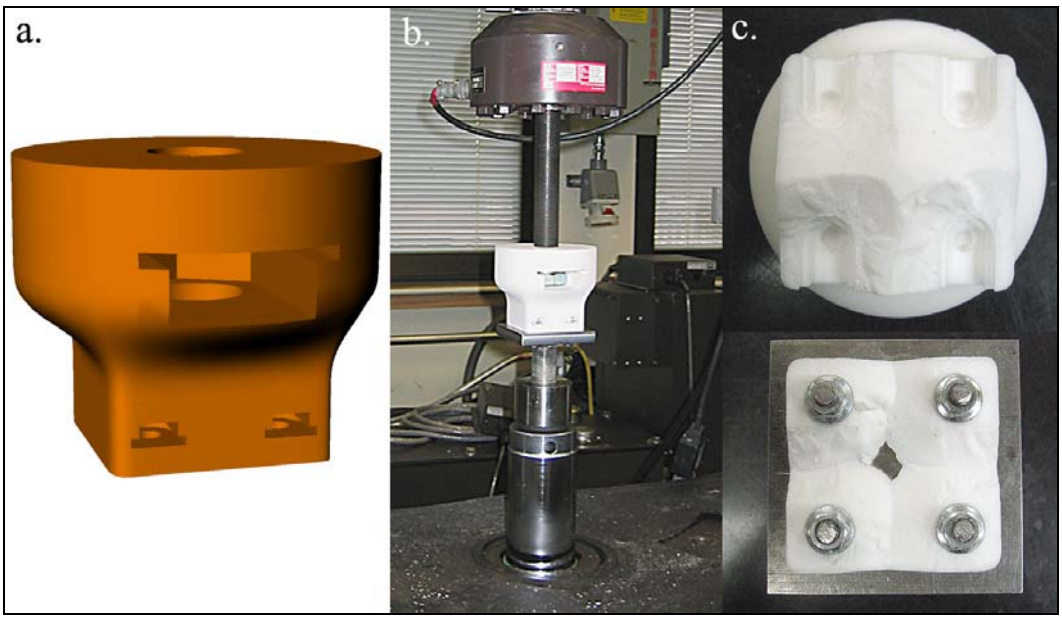

Figure 7: (a) Complete Attachment Fitting Specimen; (b) Test Setup;
(c) Specimen Condition after Testing.

Analysis of Ground Reaction Forces

The ground reaction forces are forces between the foot and the ground as a person walks. These forces are vectors with components in the *xyz* directions that are measured using an instrumented force plate. A patient wearing a prosthetic socket walks on the runway and sensors inside the force plates record the forces as the foot is in contact with the plate. The ground

reaction forces are recorded using a global coordinate system fixed to the ground. Vertical forces are represented by F_z, anterior-posterior forces by F_x, and transverse (side to side) forces by F_y (see Figure 8a for representation of the forces). These forces are recorded at the foot base, and to be useful for this research, the GRF data needs to be resolved into individual components. For the purpose of designing the attachment fitting, the most critical forces are forces that are perpendicular to the foot, since these forces create a bending moment on the socket and can cause the socket to fail. The shear forces are carried by the bolts and are not as likely to cause failure. The only GRF force that is always perpendicular to the shank is the transverse force, F_y. The vertical (F_z) and anterior-posterior (F_x) forces have both perpendicular and parallel force components (Figure 8a shows the perpendicular force components) and therefore needs to be further calculated. In order to extract the perpendicular forces, the walking angle is needed. The walking angle is defined as the angle between the shank and the ground (Figure 8b). Since the GRF data does not contain the angle information, an alternative way of incorporating the walking angle is needed.

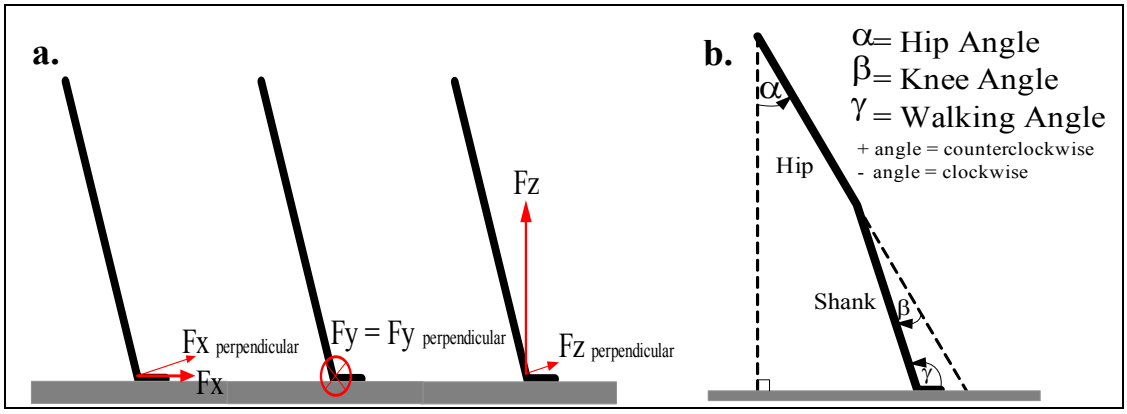

Figure 8: (a) GRF Perpendicular Forces Component;
(b) Illustration of Interpreting Waking Angle.

The method for obtaining the walking angle data is based on [6], which presents hip, knee, and ankle angles for a normal person walking. Since the interest of this study is for an amputee wearing a prosthesis, the ankle angle is not needed. Figure 8b shows how the walking angle is acquired. The hip angle (α) is the angle between the hip and vertical body movement, while the knee angle (β) is the angle between the extension of the hip and the shank. Therefore, the walking angle (γ) is the angle between the ground and the shank, and is computed as a simple function of α and β. In [6], the angle is presented over a complete gait cycle, which includes the stance and swing phases. The stance phase, which is about 65% [7] of a complete cycle, is the only phase that is needed for this analysis, so only 65% of the angle data was used.

In order to fully extract the perpendicular forces, the correlation between the GRF data and the walking angle was needed. Four sets of GRF data from amputees wearing prosthetic sockets were acquired from the UTHSCSA Gait Lab. Each person's GRF data contained 32 data points that represented forces in the *xyz* directions. For each data point, a walking angle was needed to extract the corresponding perpendicular force. Therefore, the walking angle was calculated over 32 angles.

Once walking angles were acquired, perpendicular components of vertical and anterior-posterior forces were calculated. With all the perpendicular forces known, a resultant force was then obtained by calculating the resultant of the perpendicular vertical force and anterior-posterior force. This resultant force was combined with the transverse force. The total resultant of these three forces was used to evaluate the attachment fitting under bending. A summary of the maximum for each force and the total perpendicular force is presented in Table 3.

Table 3: GRF Maximum Force.

	F_x (N)	F_y (N)	F_z (N)	Total Perpendicular Resultant Force (N)
Amputee 1	87.6	134.7	910.7	353.4
Amputee 2	79.7	107.8	638.5	257.0
Amputee 3	78.2	145.0	974.4	443.2
Amputee 4	169.4	200.6	1001.9	422.3

Relationship of GRF to Tensile Test Results

After extracting the maximum resultant forces from the GRF, the next step was correlating the forces to the test results of a complete attachment fitting. Figure 9a shows a diagram of the attachment fitting. The diagram is arranged to represent an attachment fitting, a connected adaptor, and a pylon. The results of the analysis predict whether the attachment fitting is strong enough under normal walking forces.

As indicated in Figure 9c, a bending force, which is the maximum resultant force from the GRF analysis, is applied to the end of the pylon and, as the force is applied, it will pivot at point A. F_{top} and F_{bottom} represent forces on the adaptor as the bending moment force is applied. Therefore the reaction forces from the adaptor are the tension forces that the attachment fitting experiences. The perpendicular distances between point A to the forces are represented by *a*, *b*, and *c*. Solving for the values of F_{top} and F_{bottom} gives the total tension force applied to the attachment fitting.

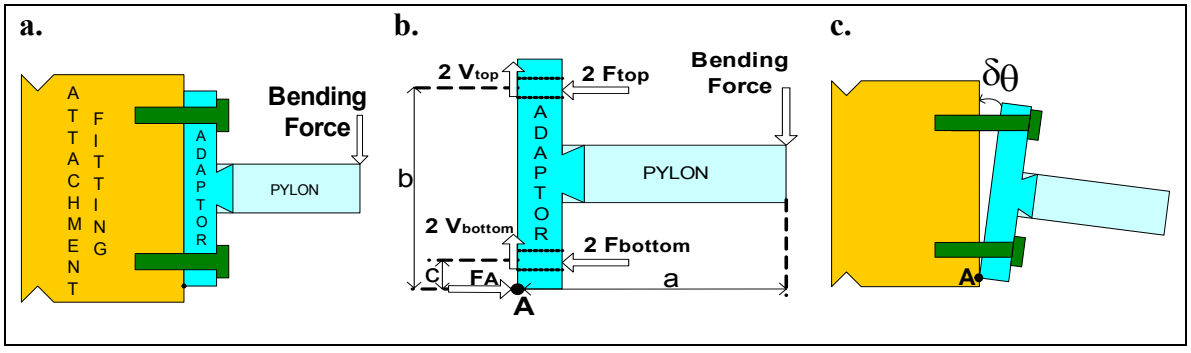

Figure 9: (a) Attachment Fitting Diagram; (b) Free Body Diagram of Attachment Fitting; (c) Rotation Angle.

From the free body diagram in Figure 9, with the adaptor tending to rotate about point A, the strains on the top and bottom bolts are

$$\delta_{Top} = b \times \delta\theta$$
$$\delta_{Bottom} = c \times \delta\theta \ ,$$

where $\delta\theta$ is the rotation angle between the bottom of the attachment fitting and the top of the adaptor. The force on each bolt is a function of the strain:

$$F_{Bolts} = f(strain)$$
$$F_{top} = f(\delta_{Top})$$
$$F_{bottom} = f(\delta_{Bottom})$$

Since $\delta\theta$ is the same for both bolts and the strains are proportional to the distances to the pivot point A, the forces can be assumed proportional:

$$F_{top} = \frac{b}{c} \times F_{bottom} \tag{1}$$

Summing the moments at point A gives

$$\sum M_A = 0$$
$$F_{bending} \times a = (2 \times F_{top} \times b) + (2 \times F_{bottom} \times c) \tag{2}$$

Solving equations (1) and (2) simultaneously for the given bending load gives the values for F_{top} and F_{bottom}. The total tensile force is then $2F_{top} + 2F_{bottom}$. The total tensile force of the attachment fitting was computed using the measured distances and maximum resultant force from GRF analysis. Table 4 summarizes the maximum tensile force the attachment fitting experiences.

Table 4: Total Tension Force of the Attachment Fitting due to Bending Force.

	F_{top} Bolt		**F_{bottom} Bolt**		**F_{total}**	
	Newton	lbf	Newton	lbf	Newton	lbf
Amputee 1	1440	324	255	57	3390	762
Amputee 2	953	214	169	38	2245	505
Amputee 3	1806	406	320	72	4252	956
Amputee 4	1567	352	278	62	3689	829

The results from the analysis show that the highest maximum tensile force applied to the attachment fitting is only 956 lbf. This force is far below the force needed to break the attachment fitting. Even though all four bolts experienced the same maximum force (in this case

4 times 406 lbf), which is 1624 lbf, the attachment fitting is still strong enough. Using the value of 1624 lbf as an upper limit for tensile force and incorporating a safety factor of 3 yields a tensile force of 4872 lbf, which is significantly smaller that the force needed to break the attachment fitting (5799.61 lbf) in the experiment. This indicates the attachment fitting will be strong enough under normal walking loads.

From the free body diagram in Figure 9b, the shear force on each of the four bolts is the same. By summing the forces in the y direction, the shear force for each bolt can be calculated as follows

$$\sum F_y = 0 \tag{3}$$
$$4 \times V_{bolt} = BendingForce$$
$$V_{bolt} = \frac{BendingForce}{4} = \frac{443.2N}{4} = 110.8N,$$

where the bending force is equal to the calculated perpendicular force in Table 4. Using the calculated values of the largest maximum tensile force in Table 4.2 and the shear force for each bolt, the equivalent stress of the bolt can be calculated using the distortion energy equation [8]:

$$\sigma_e = \sqrt{\sigma^2 + 3\tau^2}, \tag{4}$$

where the tensile stress, $\sigma = \frac{1806N}{A}$, the shear stress, $\tau = \frac{110.8N}{A}$, and A = 20.1 mm^2 for a 6mm bolt [8]. Substituting these values into equation (4) yields the equivalent stress for the bolt, which is $\sigma_e = 90.3$MPa. Incorporating a safety factor of 3 yields a tensile stress of 270.9 MPa, which means that using SAE class 4.8 bolts with a proof load of 310 MPa [8] will be sufficient to ensure that the bolts will not fail.

Conclusion

The primary result of this research is the design and testing of a new integrated attachment fitting for transtibial prosthetic sockets fabricated by selective laser sintering. The flange nut attachment fitting provides an economical, standard, and strong connection to the pylon. Flange nuts are easily obtainable and inexpensive compared to the UTHSCA design. The design should help marketability of SLS prosthetic sockets. The tensile test results and ground reaction force analysis indicate that the flange nut design is strong enough to withstand normal gait forces.

References

[1] Rogers, W. E., Crawford, R. H., Beaman, J. J., and Walsh, N. E., 1991, "Fabrication of Prosthetic Sockets by Selective Laser Sintering," 1991 Solid Freeform Fabrication Symposium Proceedings, Marcus, H. L., Beaman, J. J., Barlow, J. W., Bourell, D. L., and Crawford, R. H., eds., Austin, TX, August 12-14, 1991, pp. 158-163.

[2] Stephens, S. D., 1999, “Design of a Compliant Prosthetic Socket Fabricated Using Selective Laser Sintering,” Master’s thesis, The University of Texas at Austin, Austin, Texas.

[3] Faustini, M.C., 2004, “Modeling and Fabrication of Prosthetic Sockets using Selective Laser Sintering.” Ph.D. dissertation, The University of Texas at Austin, Austin, TX.

[4] Rogers, W. E., and Bosker, G., 2004, University of Texas Health Science Center at San Antonio, San Antonio, TX, personal interview.

[5] Firestone, K., 2004, 3D Systems, Inc., Austin, TX, personal interview.

[6] Skelly, M. M., Chizeck, H. J. “Simulation of Bipedal Walking,” [Online] Available at https://www.ee.washington.edu/techsite/papers/refer/UWEETR-2001-0001.html, August 4, 2004.

[7] Rose, J., and Gamble, J. G., 1996, “Human Walking,” Williams and Wilkins, Baltimore.

[8] Juvinall, R. C., and Marshek, K. M., 1991, “Fundamental of Machine Component Design,” John Wiley and Sons, Canada.